Inorganic Chemistry

Article

pubs.acs.org/IC

Physical Characterization and Reactivity of the Uranyl Peroxide $[UO_2(\eta^2\text{-}O_2)(H_2O)_2]\cdot 2H_2O$: Implications for Storage of Spent Nuclear Fuels

Colm Mallon,[†] Aurora Walshe,[‡] Robert J. Forster,[†] Tia E. Keyes,[†] and Robert J. Baker*[,‡]

[†]School of Chemical Sciences, Dublin City University, Dublin 9, Ireland

[‡]School of Chemistry, University of Dublin, Trinity College, Dublin 2, Ireland

ABSTRACT: The unusual uranyl peroxide studtite, $[UO_2(\eta^2\text{-}O_2)(H_2O)_2]\cdot 2H_2O$, is a phase alteration product of spent nuclear fuel and has been characterized by solid-state cyclic voltammetry. The voltammogram exhibits two reduction waves that have been assigned to the $U^{VI/V}$ redox couple at −0.74 V and to the $U^{V/IV}$ redox couple at −1.10 V. This potential shows some dependence upon the identity of the cation of the supporting electrolyte, where cations with larger ionic radii exhibit more cathodic reduction potentials. Raman spectroelectrochemistry indicated that exhaustive reduction at either potential result in a product that does not contain peroxide linkers and is likely to be UO_2. On the basis of the reduction potentials, the unusual behavior of neptunium in the presence of studtite can be rationalized. Furthermore, the oxidation of other species relevant to the long-term storage of nuclear fuel, namely, iodine and iodide, has been explored. The phase altered product should therefore be considered as electrochemically noninnocent. Radiotracer studies with ^{241}Am show that it does not interact with studtite so mobility will not be retarded in repositories. Finally, a large difference in band gap energies between studtite and its dehydrated congener metastudtite has been determined from the electronic absorption spectra.

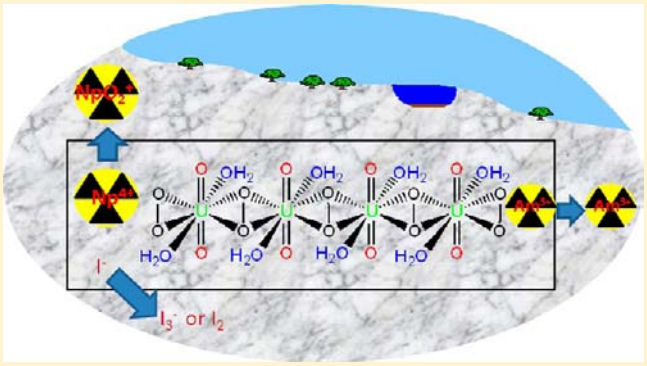

INTRODUCTION

The storage of Spent Nuclear Fuels (SNF) is a particular concern for all countries that use nuclear power to generate electricity. The European Union[1] has recommended that this should be stored in specifically engineered geological repositories, which would contain all radioactive isotopes for a time span of at least 10^6 years.[2] Under the moist, oxidizing repository conditions, the oxidation of U(IV) to U(VI) is thermodynamically favorable, so phase alterations on the surface of SNF are likely.[3] These phase alterations can have a significant impact upon the mobility of uranium and the minor actinides, but have only recently been investigated. Unirradiated UO_2[4] and SNF[5] have both been examined and the main products of alteration characterized as the uranyl oxyhydroxide minerals schoepite, $[(UO_2)_8O_2(OH)_{12}]\cdot 12H_2O$, metaschoepite, $[(UO_2)_4O(OH)_6]\cdot 5H_2O$, becquerelite, $[Ca(UO_2)_6O_4(OH)_6]\cdot 8H_2O$, and compreignacite $[K_2(UO_2)_6O_4(OH)_6]\cdot 7H_2O$, and the silicate minerals (formed by reaction of dissolved silicates in groundwater) soddyite $[(UO_2)_2(SiO_4)]\cdot 2H_2O$, uranophane $[Ca(UO_2)_2(SiO_3OH)_2]\cdot 5H_2O$, boltwoodite, $[(K,Na)(UO_2)(SiO_3OH)]\cdot 0.5H_2O$, and sklodowskite $[Mg(UO_2)_2(SiO_3OH)_2]\cdot 5H_2O$. These are layered uranyl silicates that have been compared to clay minerals[6] as they display high surface areas that are suited to radionuclide sorption.[7] Neptunium incorporation has been particularly well studied since ^{237}Np is potentially mobile with a long half-life (2.1×10^6 years),[8] but ion-exchange, for example of Cs in boltwoodite,[9] or Sr in becquerelite,[10] has also been examined. The uranyl oxyhydroxide phases, particularly schoepite and metaschoepite, also show incorporation of ^{237}Np, and those phases with interlayer cations incorporated more ^{237}Np than those without.[11]

These phases are not necessarily the thermodynamically favored alteration, as schoepite and metaschoepite are found to be replaced by studtite, $[(UO_2)(\eta^2\text{-}O_2)(H_2O)_2]\cdot 2H_2O$, over the course of two years in deionized water.[12] Further studies have shown that studtite, and its dehydration product metastudtite $[(UO_2)(\eta^2\text{-}O_2)(H_2O)_2]$, can be formed by dissolution of UO_2,[13] or the phases mentioned above,[14] in the presence of H_2O_2. Studtite has also been found on the surface of SNF,[15] "lava" from the Chernobyl Nuclear Plant accident,[16] and in naturally occurring uranium ores.[17] The formation of studtite on SNF has been ascribed to the production of H_2O_2 via alpha-radiolysis of water, and support for this comes from the observation of studtite and metastudtite upon α,[18] β,[19] and γ[20] irradiated UO_2 surfaces, and high temperature oxide-melt solution calorimetry.[21] The presence of Fe(II) ions retards formation of studtite, as decomposition of

Received: May 23, 2012
Published: July 19, 2012

   dx.doi.org/10.1021/ic3010823 | *Inorg. Chem.* 2012, 51, 8509−8515

H_2O_2 appears to be faster than precipitation of studtite.[22] The first mention of a uranium peroxide was by Fairley in 1877[23] who described the structure as containing a double peroxide. On the basis of chemical analysis and isotope exchange of ^{18}O,[24] the formulation of a hydrated uranyl bis-peroxide was suggested in 1962, and the solid state structure was determined experimentally in 2003, which is an infinite linear chain bridged by peroxides.[25] Interestingly it is the only mineral that features a peroxy group. It is worth noting that uranyl peroxides have also been formed in the presence of carbonate[26] and hydroxide[27] ions, which also have relevance to long-term storage under repository conditions. Nanoscale supramolecular clusters have been synthesized based on the uranyl peroxide template,[28] and these have been suggested as a possible speciation of uranium in the cooling tanks of the Fukushima-Daiichi nuclear reactor in Japan.[29] A computational examination of some of these smaller nanomaterials has been reported, and the bonding in these uranyl peroxides has been characterized by an overlap of U 6p orbitals with the peroxy π bond. The 6p orbitals are normally considered core-like but as the 6d and 5f orbitals are involved in bonding with the −yl oxygen, these are the next energetically accessible orbitals of the correct symmetry.[30]

It is important to determine the degree of incorporation of radionuclides into studtite and metastudtite if these are the long-term phase alteration products of SNF, particularly as environmental modeling of radionuclides that will probably be stored in geological repositories in the U.S., U.K., and other countries, have not considered leaching via these methods in detail. Cesium[31] and strontium[32] have both been shown to be sorbed onto studtite, while ^{90}Sr, ^{137}Cs, ^{99}Tc, ^{237}Np, and ^{239}Pu have been observed to concentrate in metastudtite on the basis of a 2 year immersion study of SNF.[33] Interestingly, ^{241}Am and ^{244}Cm do not concentrate to such a degree. There also appears to be a preference for ^{237}Np incorporation into metastudtite over metaschoepite (6500 ppm and <10 ppm respectively), although batch dissolution studies showed that ^{237}Np is then released into the aqueous phase.[34] The oxidation state of the neptunium in this species is uncertain, with oxidation of the initial NpO_2^+ to NpO_2^{2+} by hydrogen peroxide postulated. Quantum-mechanical calculations also suggest that incorporation of NpO_2^{2+} is energetically more favorable than NpO_2^+ in Np-studtite as it is isostructural with UO_2^{2+}.[35] Forbes et al. has interpreted this as the reduction of NpO_2^+ to insoluble Np^{4+} by the addition of H_2O_2 in the preparation of studtite and subsequent precipitation as a discrete phase, followed by gradual oxidation and release into solution.[14a] It is clear that further investigations are warranted to clarify these conflicting reports and to determine how Np and other trans-uranics are incorporated into studtite. There are three possible pathways, by (a) substitution of an isostructural UO_2^{2+} fragment; (b) sorption on the surface (as for Sr); or (c) outer-sphere redox processes. Herein we attempt to answer some of these questions by the use of solid-state electrochemistry. Solid state electrochemistry is a straightforward and versatile method pioneered by Bond and co-workers for studying redox active solid materials via their mechanical attachment to an electrode surface.[36,37] The main prerequisite is that the solid and its redox partners are not soluble in the contacting solution/electrolyte. The solid state redox reactions giving rise to the voltammetric responses are thought to occur at the solid/electrolyte/electrode interface. Heterogeneous and homogeneous electron transfer and ion transport across the solid−solvent (electrolyte) interface, and associated break in phenomena can all accompany redox transformation of the solid.[38,39] Given the potential importance of solid state redox reactions in transuranic minerals and in spent nuclear fuels, solid state electrochemistry is an attractive means of interrogating these processes. However, to our knowledge there has been only one report on the solid state electrochemistry of such materials.[40]

EXPERIMENTAL SECTION

Caution! *Natural uranium was used during the course of these experiments.* ^{241}Am *is an* α *and* γ *emitter, and all experiments were carried out in a laboratory designated for the use of radioactive isotopes.*

Studtite and meta-studtite were prepared according to the literature,[41] and all other reagents were obtained from commercial sources and used as received. $^{241}Am^{3+}$ was obtained from Amersham. UV−vis/NIR spectra were obtained using a Perkin-Elmer Lambda 1050 spectrometer with an integrating sphere, and fluorescence spectra were measured on a Horiba-Jobin-Yvon Fluorolog-3 spectrometer. Infrared spectra were recorded on a Perkin-Elmer Spectrum 100 using an Attenuated Total Internal Reflection accessory. Raman spectra were obtained on a Horiba-Jobin-Yvon HR800UV using the 633 nm line of a HeNe laser as excitation source. The laser power was adjusted to 2 mW. Cyclic voltammetry was performed on a CH Instruments Model 600 electrochemical workstation.

Solid state electrochemistry was performed in a standard three electrode configuration using a platinum mesh as a counter electrode and a Ag/AgCl (sat. KCl) reference electrode. Fluorine doped tin oxide (FDTO) coated glass was employed as the working electrode. Studtite was suspended in acetone, and the slurry mixture was dropped onto the FDTO electrode. The insolubility of studtite in aqueous solutions ensures no dissolution occurs. Although some material detaches from the electrode over the course of the measurements, this does not affect the results.

Radiotracer Experiments. $[UO_2(NO_3)_2]\cdot 6H_2O$ (0.25 g, 0.49 mmol) was dissolved in H_2O (43 cm^3) and concentrated HNO_3 (2 cm^3), and $^{241}Am^{3+}$ (5 cm^3 of a 200 kBq solution in water) was added. H_2O_2 (50 cm^3 of a 5% solution in water) was added dropwise, and the mixture was stirred for 3 days. The yellow precipitate was isolated by filtration, washed with water (2 × 20 cm^3), and dried. The sample was placed inside a calibrated Marinelli beaker and a γ-spectrum obtained.

RESULTS AND DISCUSSION

The diffuse reflectance UV−vis spectra of studtite and metastudtite are shown in Figure 1. Studtite shows an absorption edge at 360 nm, which corresponds to a band gap

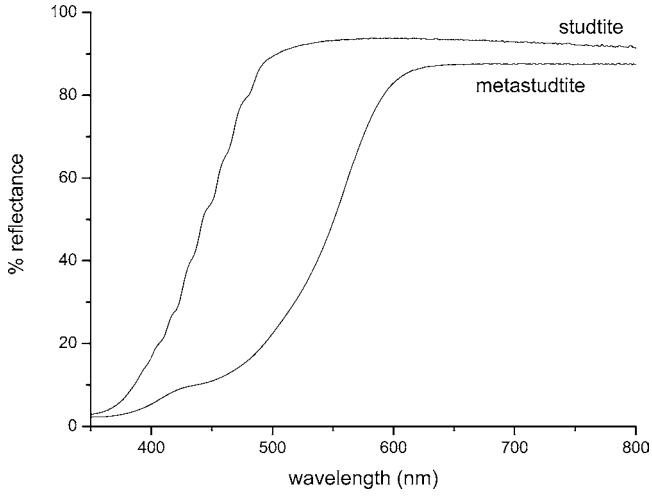

Figure 1. Diffuse reflectance UV−vis spectra of powdered studtite and metastudtite.

dx.doi.org/10.1021/ic3010823 | Inorg. Chem. 2012, 51, 8509−8515

of 3.45 eV. Somewhat surprisingly the band gap in metastudtite is 2.71 eV, 0.74 eV lower by just the removal of lattice water. The band gap for these materials has not been reported, although calculations on studtite suggest a band gap of 2.30 eV.[35,42] The electronic structures of studtite and metastudtite have been calculated, with the highest occupied molecular orbital (HOMO) of primarily $O_{peroxide}$ 2p character and the lowest unoccupied molecular orbital (LUMO) 5f in nature.[42] There is a lengthening of the U═O bond (0.018 Å) and the U−O_2 distance (0.015 Å) compared to studtite, while Raman spectroscopy also suggest little perturbation of the uranyl moiety between studtite and metastudtite.[43] It is not immediately clear where the difference arises, and we are investigating this further. For comparison, the band gaps for UO_2 and UO_3 are ∼2.0[44] and 2.17−2.83[45] (depending on the phase) eV, respectively. Conductivity measurements were thwarted by the morphology of the studtite precipitate. Interestingly, neither studtite nor metastudtite show any fluorescence in the solid state at room temperature or at 77 K. This is of note as the uranyl moiety is normally a strong emitter,[46] although carbonate ligands[47] and coordinated water[48] can quench the emission. Given the calculations on the electronic structure, we postulate that quenching occurs either via fast energy transfer to the peroxy group or, more likely, vibrational quenching via the coordinated water molecules.

Solid State Electrochemistry. Solid state voltammetry was employed to determine the electrochemical activity of studtite. Figure 2 shows cyclic voltammograms (CVs) of a solid

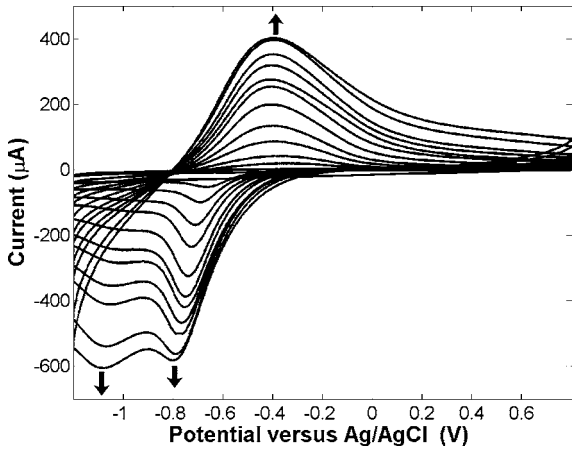

Figure 2. CVs of studtite on FDTO in water with 0.2 M $LiClO_4$ as the supporting electrolyte (scan rate = 0.1 V s^{-1}).

deposit of studtite at FDTO electrodes in contact with water containing 0.2 M $LiClO_4$ as the supporting electrolyte at a scan rate of 0.1 V s^{-1}. During the initial potential cycles, little faradaic current is observed but gradually a reduction peak appears at approximately −0.73 V, which through potential bracketing experiments was found to be linked to the oxidative process at −0.35 V. The intensity of the voltammetric waves increases with increasing number of scans, over a period of several hours. A second reduction peak becomes evident at −1.10 V with a coupled oxidation process which overlaps with the previous oxidative process to give a broad peak centered at −0.4 V. The second reduction process shows a slower current increase compared to the reduction at −0.73 V, but both peaks stabilize at similar current values. As the film is reduced, it is expected to incorporate electrolyte ions to maintain charge stability. The gradual increase of the peaks in the CV is attributable to improved penetration of ions through the film, as the morphology of the film is changed with time. As these films are quite thick, that is, 1−5 μm, ion diffusion presumably limits the amount of current observed until the film becomes saturated with ions. Interestingly, ion incorporation appears to be driven solely by the electrochemical process, as contact with 0.2 M $LiClO_4$ electrolyte over 24 h without applying potential did not decrease the "break-in" time in subsequent electrochemical measurements.

The electrochemical characteristics of studtite films on FDTO were investigated in a variety of electrolytes, namely, $LiClO_4$, $NaClO_4$, $KClO_4$, and Na_2SO_4, to probe the effect of both cation and anion identity on the electrochemical behavior of the film. Electrochemistry performed in the presence of the above electrolytes gave rise to CVs with shapes and break in characteristics very similar to those presented in Figure 2. However, the potential of the first reduction showed a weak dependence on the cation employed. In 0.2 M $LiClO_4$ the first reduction occurs at a potential of −0.73 V, while in 0.2 M $NaClO_4$ this value shifts to −0.76 V and in 0.2 M $KClO_4$ it occurs at −0.79 V. In contrast, the first reduction occurred at a potential of −0.76 V in 0.2 M Na_2SO_4, indicating that the anion has little influence on the film's electrochemical properties. The increasingly cathodic reduction potentials observed with increasing cation size suggests cation diffusion is a limiting factor in film electrochemistry. This behavior is consistent with the "break-in" phenomenon observed leading to the appearance of voltammetric waves, as it suggests that the electrochemistry is driving ion transport. Since the film is being reduced it is unsurprising that cation rather than anion transport is the limiting factor. The results conform well with a related study by Bond et al. on solid state voltammetry of uranium oxides mechanically attached to graphite electrodes which also indicated U^{VI} to U^{V} electron transfer coupled to cation diffusion leading to topochemical insertion compound at the solid electrode−electrolyte interface.[40] Therefore, all subsequent experiments were carried out using $LiClO_4$ as the electrolyte. Table 1 shows selected literature values for the

Table 1. U^{VI}/U^{V} Redox Couples for Selected Uranyl Compounds (vs Ag/AgCl)

compound	solvent[a]	E_{red} (V)	reference
$[UO_2(O_2)(H_2O)_2]\cdot 2H_2O$	solid-state	−0.76	this work
$[UO_2(H_2O)_5]^{2+}$	H_2O	−0.68	51
$[UO_2(dmso)_5]^{2+}$	DMSO	−1.71	52
$[UO_2(acac)_2(DMSO)]$	DMSO	−2.19	53
$[UO_2Cl_4]^{2-}$	H_2O	−0.065	54
$[UO_2Cl_4]^{2-}$	$EMI^+BF_4^-/Cl^-$	−1.72	55
$[U(CO_3)_5]^{6-}$	H_2O	−1.20	56
$[UO_2(CO_3)_3]^{4-}$	H_2O	−0.86	57

[a]EMI = 1-ethyl-3-methylimidazolium.

reduction of U^{VI} to U^{V} in various U containing compounds. Clearly a wide variety of redox potentials are observed, but there is a growing body of evidence that suggests the redox couple is mainly dependent on the π-donation of the ligand which can mix with 6d orbitals on uranium thus stabilizing higher oxidation states, while ligand denticity and solvation effects play a more subtle role.[49] Thus the more π-donating the ligand, the more negative the $U^{VI/V}$ redox couple. This is also supported by a correlation between the $U^{VI/V}$ redox potential

dx.doi.org/10.1021/ic3010823 | Inorg. Chem. 2012, 51, 8509−8515

and the symmetric U=O stretch in the Raman spectrum.[50] Our measurements in the solid state are broadly in agreement. It is also generally agreed that the $U^{VI/V}$ couple is quasi-reversible but that U^{V} species undergo disproportionation to U^{VI} and U^{IV}.[50] Therefore, based on these values the first reduction at −0.73 V, which couples to the oxidation observed at −0.35 V observed in Figure 2, is tentatively attributed to the $U^{VI/V}$ couple. This is also consistent with calculations which indicate the LUMO is of U 5f orbital character.[42]

Varying the time scale of the electrochemical experiment can provide valuable information on the movement of charge within the film. Under semi-infinite diffusion conditions, the Randles−Sevcik equation (eq 1) can be applied to determine the diffusion of charge transport, D_{CT}, within the film:

$$i_p = 2.69 \times 10^5 \cdot n^{3/2} \cdot A \cdot {D_{CT}}^{1/2} \cdot C \cdot \nu^{1/2} \quad (1)$$

where i_p is the peak current, n is the number of electrons transferred, A is the area of the electrode, C is the concentration of redox centers in the film, and ν is the scan rate. Figure 3

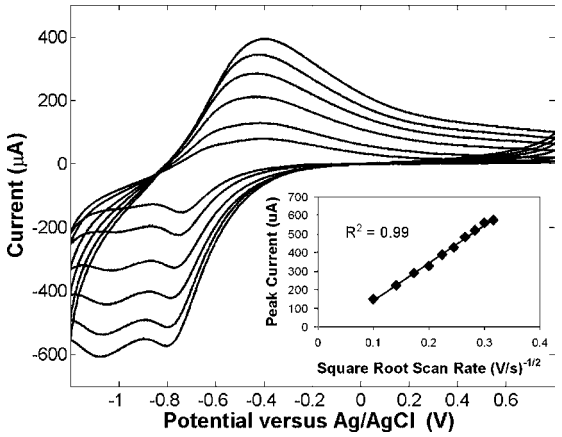

Figure 3. CVs of studtite on FDTO in water with 0.2 M $LiClO_4$ as the supporting electrolyte at scan rates of 0.01, 0.02, 0.04, 0.06, 0.08, 0.1 V s^{-1} (from low to high current). The inset shows the relationship between the peak current and the scan rate over this range for the first reduction.

shows CVs of studtite on FDTO in 0.2 M $LiClO_4$ at scan rates from 10 to 100 mV s^{-1}. The inset of this figure shows a plot of the peak current for the first reduction wave versus the square root of the scan rate, and a linear trend is clearly observed. Therefore, between these measured scan rates the diffusion characteristics are consistent with a semi-infinite diffusion model, and eq 1 can be used to calculate D_{CT}. The concentration of redox centers (i.e., uranium atoms) in the film can be calculated from the crystallographic parameters[25] as 2.5 M. Assuming the first reduction is the $U^{VI/V}$ couple (i.e., n = 1), a D_{CT} of 1.2 ± 0.4 × 10^{-11} cm^2 s^{-1} can be calculated. This value is the limiting charge transfer step, typically because of the movement of either electrons or ions through the film. Ion diffusion coefficients for other minerals are typically lower than the value reported here,[58] perhaps suggesting that the D_{CT} is dominated by ion movement.

Figure 3 also shows that magnitude of the second reduction peak at −1.10 V relative to the first reduction at −0.73 V is dependent on the scan rate. The overlap of the oxidative processes for these couples prevents definite comparison but at fast scan rates the peak current of the two reductive processes are similar, suggesting that an equal number of electrons are transferred in each step. This strongly suggests that each step is a one electron transfer. As the peroxide reduction is a two electron process, this would imply that the second reduction at −1.10 V is due to reduction of the chemically unstable U^{V} product from the first step to U^{IV}. Therefore, the diminished magnitude of the second reduction peak relative to the first reduction peak may be due to a chemical reaction following the initial electrochemical reduction of the U^{VI} to U^{V} (an EC mechanism) which depletes the amount of U^{V} species present; this has been noted previously.[56] Furthermore, the exhaustive reduction of the studtite layer has been studied at −0.9 V and at −1.2 V for 12 h, that is, after both the first and the second reduction peak, respectively, to determine the effect of each reduction on the studtite film. Interestingly, the studtite film, which is yellow before reduction, turns brown-black after exhaustive electrolysis at *both* potentials; this type of color change has been observed in reduction of uranyl nitrate in imidazolium based ionic liquids and was ascribed to the formation of UO_2.[59]

Figure 4 shows the Raman spectra of a solid deposit of studtite on FDTO, before and after 12 h bulk electrolysis at

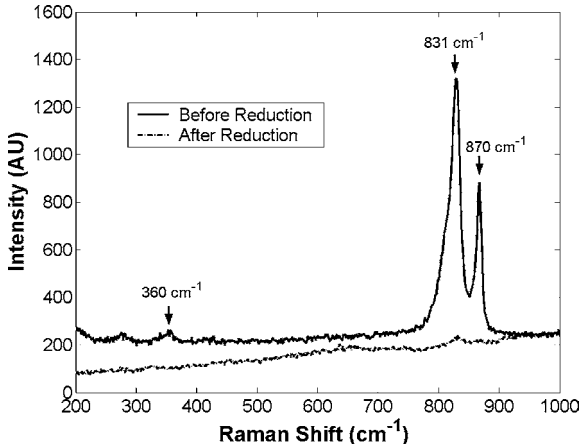

Figure 4. Raman spectra of studtite on FDTO before and after reduction at −1.2 V for 12 h in 0.2 M $LiClO_4$. The excitation line is 633 nm.

−1.2 V following exhaustive cycling. Identical spectra are obtained for the material created by reduction at −1.2 V and −0.9 V. Prior to electrolysis, the Raman spectrum for the studtite sample conforms well to that reported previously, and is dominated by the symmetric uranyl (υ_s U=O) stretch at 831 cm^{-1} and the stretch (υO−O) of the bridging peroxo ligands at 870 cm^{-1}.[43] Finally a weak (υ_{as}U−O) peroxo mode is observed at approximately 360 cm^{-1}. In contrast, the electrolysis products generated at *either* −1.2 V or −0.9 V are almost silent in the range 200 to 1000 cm^{-1}; a weak feature appears at 831 cm^{-1} attributed to unelectrolyzed material. The product is almost black in color which will affect its ability to scatter 633 nm excitation. This is consistent with a report on Raman spectra of UO_2 which found this material to be a very poor Raman scatterer under red irradiation.[60] Nonetheless, it seems clear on the basis of the loss of the associated Raman features that reduction results in the cleavage of the peroxide linkers of the material. This is consistent with the hypothesis that the first reduction involves reduction to U^{V} which would then spontaneously disproportionate to U^{IV} and U^{VI}, while the

dx.doi.org/10.1021/ic3010823 | Inorg. Chem. 2012, 51, 8509−8515

second reduction involves the reduction of U^{V} to U^{IV} electrochemically. Therefore, the final product is likely to contain U^{IV} and no peroxide linkers.

Raman spectroscopy indicates major and irreversible structural change to the studtite on electrolysis. This would be expected to result in significant differences to the morphology of the film. Figure 5 shows SEMs of the FDTO

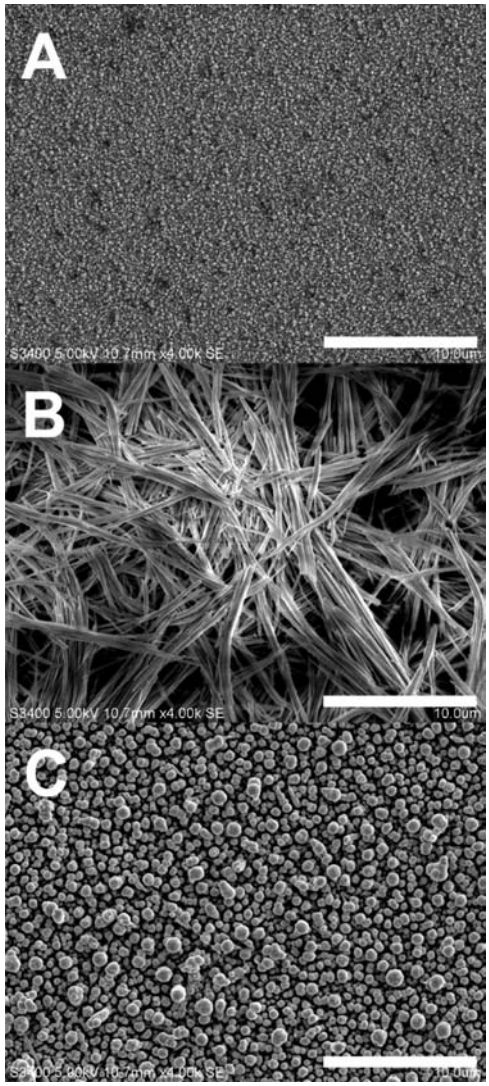

Figure 5. SEMs of (A) bare FDTO, (B) studtite on FDTO, and (C) B after reduction at −1.2 V for 12 h in 0.2 M $LiClO_4$ after exhaustive cycling.

surface (A), the studtite film (B), and the reduced product (C). Figure 5A shows that the bare FDTO surface is relatively featureless. However, Figure 5B shows that the deposited studtite forms a highly fibrous layer on the electrode surface, with significant pore openings between the strands, which are several micrometers in length. In contrast, Figure 5C shows that after exhaustive reduction the layer undergoes a complete morphological change to a granular structure, in which the grain size is approximately 0.5−1 μm. Similar to the Raman studies, this morphological change is identical for electrolysis at −1.2 V and −0.9 V. This dramatic change in the feature shape clearly demonstrates that a large change occurs to the deposited studtite during reduction, which is consistent with conversion of the material to a new chemical species as indicated by Raman spectroscopy. The significant morphology change may have important implications for the surface chemistry of SNF in terms of radionuclide mobility and further reactivity. EDX measurements on the reduced product indicate that it is composed of uranium and oxygen, that is, no new atoms are found. These considerations suggest that the reduced product may be UO_2. Unfortunately we have been unable to measure the powder X-ray diffraction patterns of the small amount of material we obtain under our electrochemical conditions. If the reduced product is left in air for a period of time the color changes to yellow; this is indicative of reoxidation to U^{VI}.

From our cyclic voltammetry measurements we can now comment upon the behavior of neptunium in the aforementioned batch dissolution studies.[33] The redox potential of $Np^{V/IV}$ in acidic media is reported to be +0.801 V while for $Np^{VI/V}$ it is +1.356 V (vs. Ag/AgCl).[61] Therefore, the oxidation of Np^{IV} to Np^{V} and concomitant reduction of the uranyl to UO_2 in studtite will be favorable. This supports the proposition of Forbes et al. that Np^{V} is initially reduced to Np^{IV} by H_2O_2 followed by slow oxidation to the soluble Np^{V}.[14a] Therefore studtite can be considered as electrochemically noninnocent, and should be borne in mind in the modeling of actinide ion migrations from SNF repositories.

■ REACTION STUDIES

Guided by our cyclic voltammetry studies, we have examined the reaction of a number of ions relevant to the nuclear fuel cycle with studtite. ^{129}I is a long-lived fission product ($t_{1/2}$ = 1.57×10^7 years) that directly affects metabolic processes and is a cause for serious environmental and toxicological concern. Moreover, ^{129}I contamination at the Savannah River[62] and Hanford[63] sites in the U.S. has been measured, and remediation techniques are required.[64] In the terrestrial environment iodide, iodine and iodate are the common oxidation states as well as organic iodine. Recent work has shown that MOFs[65] and Ag impregnated zeolites[66] show promise for removal of iodine, while birnessite (MnO_2 minerals) can oxidize I^- to I_2 and IO_3.[67] The redox potential of I_2 oxidation to IO_3^- is reported to be +1.19 V, so outside the electrochemical window of the $U^{VI/V}$ redox couple in studtite and when a solution of I_2 was contacted with studtite or metastudtite, no oxidation or sorption was observed by monitoring with UV−vis spectroscopy. Iodide was also investigated as the redox potential of the I^-/I^{3-} redox couple is 0.733 V (vs Ag/AgCl).[68] In this case we observe an oxidation to I_3^- over a period of one week; a control experiment without studtite showed no formation of I_3^- under the same conditions. We therefore suggest that I^- is slowly oxidized to I^{3-} with concomitant reduction of U^{VI}. Further oxidation of I^{3-} to I_2 (E_{red} = 0.31 V (vs Ag/AgCl) is not observed, even in the presence of excess studtite.

If this postulate that an outer-sphere redox process is important for neptunium incorporation, then a study of Pu and Am would be insightful. The redox chemistry of plutonium in all its oxidation states is complex, but the $[PuO_2]^{2+}$ ion is relatively stable. Am^{III} has redox processes outside the studtite window and the americyl ion is rather unstable, so we would predict that redox reactions would not occur. We were unable to conduct any Pu experiments in our laboratory, but tracer studies with ^{241}Am are possible. The solution chemistry of Am is not as complex as plutonium,[61,69] and in acidic solutions Am^{3+} and AmO_2^{2+} are the only stable species. Under the conditions of our experiment, it is likely that only Am^{3+} will be

dx.doi.org/10.1021/ic3010823 | Inorg. Chem. 2012, 51, 8509−8515

in solution. Addition of a tracer solution of Am^{3+} to the reaction mixture of uranyl nitrate, nitric acid, and hydrogen peroxide afforded a yellow precipitate after stirring for 3 days. This precipitate was isolated and washed with water before drying, and the gamma-spectrum measured for the typical ^{241}Am gamma emission at 58.54 keV (Figure 6). Less than 1

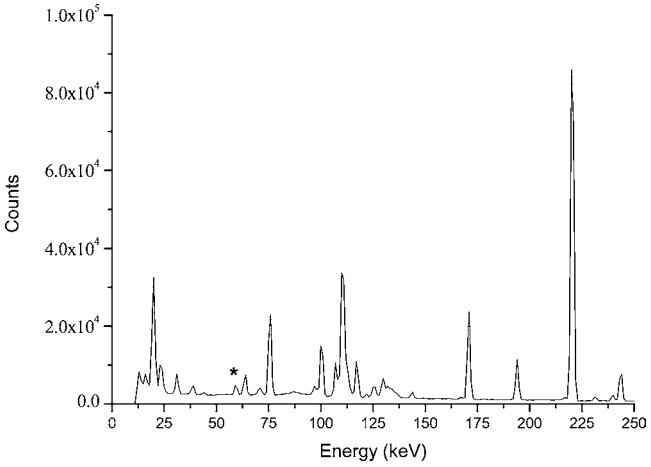

Figure 6. γ-spectrum of ^{241}Am tracer experiment. ^{241}Am emission is marked with an *. Other peaks are due to daughter products from ^{235}U and ^{238}U decay.

Bq/g of ^{241}Am was incorporated or sorbed onto studtite. This is in keeping with the results of SNF analysis,[33] and therefore suggests that retarded mobility of americium by studtite will be small.

CONCLUSIONS

In conclusion, we have characterized studtite by a number of techniques. Solid-State cyclic voltammetry has shown two redox waves assigned to a reduction to $U^{VI/V}$ and $U^{V/IV}$ redox couples. The potentials of these processes show dependence on cation but not anion identity, indicating cation ingress/egress from the film accompanies the redox processes. Potential scan rate dependence demonstrated a linear dependence of peak current on the square root scan rate indicating semi-infinite diffusion into the film and diffusion coefficient of D_{CT} of $1.2 \pm 0.4 \times 10^{-11}$ cm^2 s^{-1} in the presence of aqueous 0.2 M $LiClO_4$ as electrolyte. Exhaustive reduction at both potentials causes decomposition of studtite to what we presume is UO_2. The common fission product I_2 has been investigated and is not removed from solution upon contact with studtite or metastudtite; oxidation of I^- to I^{3-} was however observed. Radiotracer studies using ^{241}Am showed no sorption behavior. Finally, the band-gaps for studtite and its dehydrated congener have been measured and a difference noted, as might be predicted by the color difference in these two compounds. This work demonstrates that the phase altered product studtite is electrochemically active and could account for the unusual reactivity previously observed with neptunium. Moreover, it highlights that these phase altered materials should be included in long-term studies on the storage of spent nuclear fuel.

AUTHOR INFORMATION

Corresponding Author

*Phone: +353-1-8963501. Fax: +353-1-6712826. E-mail: bakerrj@tcd.ie.

Notes

The authors declare no competing financial interest.

ACKNOWLEDGMENTS

R.J.B. and A.W. thank IRCSET for funding through the EMBARK Initiative, and C.M., R.J.F., and T.E.K. gratefully acknowledge SFI for funding under PI award Grant [10/IN.1/B3025] and the National Biophotonics and Imaging Platform initiative funded under the HEA Programme for Research in Third-Level Institutions - Cycle 4. Dr. Louis León Vintró (University College, Dublin) is thanked for measuring the γ-spectrum of ^{241}Am tracer experiments.

REFERENCES

(1) Falck, W. E.; Nilsson, K.-F. Geological disposal of radioactive waste: moving towards implementation. Joint Research Centre Reference Report, EUR23925; European Commission: Luxembourg, 2009.

(2) Choppin, G.; Liljenzin, J.-O.; Rydberg, J. *Radiochemistry and Nuclear Chemistry*, 3rd ed.; Butterworth-Heinemann: Woburn, MA, 2002.

(3) Johnson, L. H.; Shoesmith, D. W. In *Radioactive Waste Forms for the Future*; Lutze, W., Ewing, R. C., Eds.; Elsevier: New York, 1988; pp 635−698.

(4) (a) Wronkiewicz, D. J.; Bates, J. K.; Wolf, S. F.; Buck, E. C. *J. Nucl. Mater.* **1996**, *238*, 78−95. (b) Wronkiewicz, D. J.; Bates, J. K.; Gerding, T. J.; Veleckis, E.; Tani, B. S. *J. Nucl. Mater.* **1992**, *190*, 107−127.

(5) (a) Finch, R. J.; Buck, E. C.; Finn, P. A.; Bates, J. K. *Mater. Res. Soc. Symp. Proc.* **1999**, *556*, 431−438. (b) Finn, P. A.; Hoh, J. C.; Wolf, S. F.; Slater, S. A.; Bates, J. K. *Radiochim. Acta* **1996**, *74*, 65−71.

(6) Wall, N. A.; Clark, S. B.; McHale, J. L. *Chem. Geol.* **2010**, *274*, 149−157.

(7) Parker, A., Rae, J. E., Eds.; *Environmental Interactions of Clays: Clays and the Environment*; Springer-Verlag: Berlin, Germany, 2010.

(8) (a) Klingensmith, A. L.; Burns, P. C. *Am. Mineral.* **2007**, *92*, 1946−1951. (b) Douglas, M.; Clark, S. B.; Friese, J. I.; Arey, B. W.; Buck, E. C.; Hanson, B. D.; Utsunomiya, S.; Ewing, R. C. *Radiochim. Acta* **2005**, *93*, 265−272. (c) Burns, P. C.; Deely, K. M.; Skanthakumar, S. *Radiochim. Acta* **2004**, *92*, 151−159.

(9) Burns, P. C. *J. Nucl. Mater.* **1999**, *265*, 218−223.

(10) Burns, P. C.; Li, Y. *Am. Mineral.* **2002**, *87*, 550−557.

(11) (a) Klingensmith, A. L.; Deely, K. M.; Kinman, W. S.; Kelly, V.; Burns, P. C. *Am. Mineral.* **2007**, *92*, 662−669. (b) Fortner, J. A.; Finch, R. J.; Kropf, A. J.; Cunnane, J. C. *Nucl. Technol.* **2004**, *148*, 174−180. (c) Burns, P. C.; Deely, K. M.; Skanthakumar, S. *Radiochim. Acta* **2004**, *92*, 151−159. (d) Buck, E. C.; Finch, R. J.; Finn, P. A.; Bates, J. K. In *Proceedings of the 21st International Symposium on the Scientific Basis for Nuclear Waste Management*, Davos, Switzerland, Sep 28−Oct 3, 1997; McKinley, I. G., McCombie, C., Eds.; RILEM Publications SARL: Bagneux, France, 1997; pp 87−94.

(12) (a) Hanson, B.; McNamara, B.; Buck, E.; Friese, J.; Jenson, E.; Krupka, K. *Radiochim. Acta* **2005**, *93*, 159−169. (b) McNamara, B.; Buck, E.; Hanson, B. *Mater. Res. Soc. Symp. Proc.* **2002**, *757*, 401−406.

(13) (a) Kim, K.-W.; Hyun, J.-T.; Lee, K.-Y.; Lee, E.-H.; Lee, K.-W.; Song, K.-C.; Moon, J.-K. *J. Hazard. Mater.* **2011**, *193*, 52−58. (b) Clarens, F.; de Pablo, J.; Casas, I.; Giménez, J.; Rovira, M.; Merino, J.; Cera, E.; Bruno, J.; Quiñones, J.; Martínez-Esparza, A. *J. Nucl. Mater.* **2005**, *345*, 225−231. (c) Clarens, F.; de Pablo, J.; Díez, I.; Casas, I.; Giménez, J.; Rovira, M. *Environ. Sci. Technol.* **2004**, *38*, 6656−6661. (d) Amme, M.; Renker, B.; Schmid, B.; Feth, M. P.; Bertagnolli, H.; Döbelin, W. *J. Nucl. Mater.* **2002**, *306*, 202−212. (e) Diaz-Arocas, P.; Quinones, J.; Maffiotte, C.; Serrano, J.; Garcia, J.; Almazan, J. R.; Esteban, J. *Mater. Res. Soc. Symp. Proc.* **1995**, *353*, 641−648.

(14) (a) Forbes, T. Z.; Horan, P.; Devine, T.; McInnis, D.; Burns, P. C. *Am. Mineral.* **2011**, *96*, 202−206. (b) Finch, R. J.; Ewing, R. C. *Mater. Res. Soc. Symp. Proc.* **1994**, *333*, 625−630.

(15) Abrefah, J.; Marschmann, S.; Jenson, E. D. *PNNL-11806*; Pacific Northwest National Laboratory: Richland, WA, 1998.
(16) Burakov, B. E.; Strykanova, E. E.; Anderson, E. B. *Mater. Res. Soc. Symp. Proc.* **1997**, *465*, 1309−1311.
(17) (a) Čejka, J.; Sejkora, J.; Deliens, M. *Neues Jahrb. Mineral. Monatsh.* **1996**, 125−134. (b) Deliens, M.; Piret, P. *Am. Mineral.* **1983**, *68*, 456−458. (c) Walenta, K. *Am. Mineral.* **1974**, *59*, 166−711.
(18) Sattonnay, G.; Ardois, C.; Corbel, C.; Lucchini, J. F.; Barthe, M.-F.; Garrido, F.; Gosset, D. *J. Nucl. Mater.* **2001**, *288*, 11−19.
(19) Clarens, F.; Giménez, J.; de Pablo, J.; Casas, I.; Rovira, M.; Dies, J.; Quiñones, J.; Martínez-Esparza, A. *Radiochim. Acta* **2005**, *93*, 533−538.
(20) Jegou, C.; Muzeau, B.; Broudic, V.; Peuget, S.; Poulesquen, A.; Roudil, D.; Corbel, C. *J. Nucl. Mater.* **2005**, *341*, 62−82.
(21) Hughes Kubatko, K.-A.; Helean, K. B.; Navrotsky, A.; Burns, P. C. *Science* **2003**, *302*, 1191−1193.
(22) Amme, M.; Bors, W.; Michel, C.; Stettmaier, K.; Rasmussen, G.; Betti, M . *Environ. Sci. Technol.* **2005**, *39*, 221−229.
(23) Fairley, T. *J. Chem. Soc.* **1877**, *31*, 125−143.
(24) (a) Lonadier, F. D.; Boggs, J. E. *J. Less Common Met.* **1963**, *5*, 112−116. (b) Porte, A. L.; Gutowsky, H. S.; Boggs, J. E. *J. Chem. Phys.* **1962**, *37*, 2318−2322.
(25) Burns, P. C.; Hughes, K.-A. *Am. Mineral.* **2003**, *88*, 1165−1168.
(26) (a) Kim, K.-W.; Kim, Y.-H.; Lee, S.-Y.; Lee, J.-W.; Joe, K.-S.; Lee, E.-H.; Kim, J.-S.; Song, K.; Song, K.-C. *Environ. Sci. Technol.* **2009**, *43*, 2355−2361. (b) Goff, G. S.; Brodnax, L. F.; Cisneros, M. R.; Peper, S. M.; Field, S. E.; Scott, B. L.; Runde, W. H. *Inorg. Chem.* **2008**, *47*, 1984−1990.
(27) Meca, S.; Martínez-Torrents, A.; Martí, V.; Giménez, J.; Casas, I.; de Pablo, J. *Dalton Trans.* **2011**, *40*, 7976−7982.
(28) Burns, P. C.; Ikeda, Y.; Czerwinski, K. *MRS Bull.* **2010**, *35*, 868−876.
(29) Armstrong, C. R.; Nyman, M.; Shvareva, T.; Sigmon, G. E.; Burns, P. C.; Navrotsky, A. *Proc. Natl. Acad. Sci. U.S.A.* **2012**, *109*, 1874−1877.
(30) Vlaisavljevich, B.; Gagliardi, L.; Burns, P. C. *J. Am. Chem. Soc.* **2010**, *132*, 14503−14508.
(31) Giménez, J.; Martínez-Lladó, X.; Rovira, M.; de Pablo, J.; Casas, I.; Sureda, R.; Martínez-Esparza, A. *Radiochim. Acta* **2010**, *98*, 479−483.
(32) Sureda, R.; Martínez-Lladó, X.; Rovira, M.; de Pablo, J.; Casasa, I.; Giménez, J. *J. Hazard. Mater.* **2010**, *181*, 881−885.
(33) McNamara, B.; Hanson, B.; Buck, E.; Soderquist, C. *Radiochim. Acta* **2005**, *83*, 169−175.
(34) Douglas, M.; Clark, S. B.; Friese, J. I.; Arey, B. W.; Buck, E. C.; Hanson, B. D. *Environ. Sci. Technol.* **2005**, *39*, 4117−4124.
(35) Shuller, L. C.; Ewing, R. C.; Becker, U. *Am. Mineral.* **2010**, *95*, 1151−1160.
(36) Nafadya, A.; Bond, A .M.; Bilyk, A.; Harris, A. R.; Bhatt, A. I.; O'Mullane, A. P.; De Marco, R. *J. Am. Chem. Soc.* **2007**, *129*, 2369−2382.
(37) Bond, A. M.; Colton, R.; Daniels, F.; Fernando, D. R.; Marken, F.; Nagaosa, Y.; Van Steveninck, R. F. M.; Walter, J. N. *J. Am. Chem. Soc.* **1993**, *115*, 9556−9562.
(38) Bond, A. M.; Marken, F.; Williams, C. T.; Beatty, D.; Keyes, T. E.; Forster, R. J.; Vos, J. G. *J. Phys. Chem. B* **2000**, *104*, 1977−1983.
(39) Keyes, T. E.; Forster, R. J.; Bond, A. M.; Miaou, W. *J. Am. Chem. Soc.* **2001**, *123*, 2877−2884.
(40) Dueber, R. E.; Bond, A. M.; Dickens, P. G. *J. Electrochem. Soc.* **1992**, *139*, 2363−2371.
(41) Debets, P. C. *J. Inorg. Nucl. Chem.* **1963**, *35*, 727−730.
(42) Ostanin, S.; Zeller, P. *Phys. Rev. B: Condens. Matter* **2007**, *75*, 073101.
(43) Bastians, S.; Crump, G.; Griffith, W. P.; Withnall, R. *J. Raman Spectrosc.* **2004**, *35*, 726−731.
(44) Winter, P. W. *J. Nucl. Mater.* **1989**, *161*, 38−43.
(45) Hanafi, Z. M.; Ismail, F. M.; Khilla, M. A.; Rofail, N. H. *Radiochim. Acta* **1990**, *49*, 35−37.
(46) (a) Geipel, G. *Coord. Chem. Rev.* **2006**, *250*, 844−854. (b) Denning, R. G. *Struct. Bonding (Berlin)* **1992**, *79*, 215−276. (c) Beitz, J. V.; Bowers, D. L.; Doxtader, M. M.; Maroni, V. A.; Reed, D. T. *Radiochim. Acta* **1988**, *44−45*, 87−93.
(47) Balzani, V.; Bolleta, F.; Gandolfi, M. T.; Maestri, M. *Top. Curr. Chem.* **1978**, *75*, 1−64.
(48) Kimura, T.; Nagaishi, R.; Kato, Y.; Yoshida, Z. *Radiochim. Acta* **2001**, *89*, 125−130.
(49) (a) Hardwick, H. C.; Royal, D. S.; Helliwell, M.; Pope, S. J. A.; Ashton, L.; Goodacre, R.; Sharrad, C. A. *Dalton Trans.* **2011**, *40*, 5939−5952. (b) Clark, D. L.; Conradson, S. D.; Donohoe, R. J.; Keogh, D. W.; Morris, D. E.; Palmer, P. D.; Rogers, R. D.; Tait, C. D. *Inorg. Chem.* **1999**, *38*, 1456.
(50) Fortier, S.; Hayton, T. W. *Coord. Chem. Rev.* **2010**, *254*, 197−214.
(51) Austin, J. P.; Sundararajan, M.; Vincent, M. A.; Hillier, I. H. *Dalton Trans.* **2009**, 5902−5909.
(52) Kim, S.-Y.; Tomiyasu, H.; Ikeda, Y. *J. Nucl. Sci. Technol.* **2002**, *39*, 160−165.
(53) Lee, S.-H.; Mizuguchi, K.; Tomiyasu, H.; Ikeda, Y. *J. Nucl. Sci. Technol.* **1996**, *33*, 190−192.
(54) Morris, D. E. *Inorg. Chem.* **2002**, *41*, 3542−3547.
(55) Ogura, T.; Takao, K.; Sasaki, K.; Arai, T.; Ikeda, Y. *Inorg. Chem.* **2011**, *50*, 10525−10527.
(56) Hennig, C.; Ikeda-Ohno, A.; Emmerling, F.; Kraus, W.; Bernhard, G. *Dalton Trans.* **2010**, *39*, 3744−3750.
(57) Mizuguchi, K.; Park, Y.-Y.; Tomiyasu, H.; Ikeda, Y. *J. Nucl. Sci. Technol.* **1993**, *30*, 542−548.
(58) Brady, J. B.; Cherniak, D. J. *Rev. Mineral GeoChem.* **2010**, *72*, 899−920.
(59) Bradley, A. E.; Hardacre, C.; Nieuwenhuyzen, M.; Pitner, W. R.; Sanders, D.; Seddon, K. R.; Thied, R. C. *Inorg. Chem.* **2004**, *43*, 2503−2514.
(60) Senanayake, S. D.; Rousseau, R.; Colegrave, D.; Idriss, H. *J. Nucl. Mater.* **2005**, *342*, 179−187.
(61) Runde, W. H.; Schulz, W. W. In *The Chemistry of the Actinide and Transactinide Elements*, 4th ed.; Morss, L. R., Edelstein, N. M., Fuger, J., Eds.; Springer: Dordrecht, The Netherlands, 2010.
(62) Denham, M. E. *Potential in-situ remediation of 129I and 99Tc in groundwater associated with the F-area seepage basins (U)*. WSRC-TR-2002-00571. Westinghouse Savannah River Co.: Aiken, SC, 2002.
(63) Riley, R. G.; Zachara, J. M. *Nature of Chemical Contaminants on DOE Lands and Identification of Representative Contaminant Mixtures for Basic Subsurface Science Research*, Rept. DOE/ER-547T; U.S. Department of Energy, 1992.
(64) Xu, C.; Miller, E. J.; Zhang, S.; Li, H.-P.; Ho, Y.-F.; Schwehr, K. A.; Kaplan, D. I.; Otosaka, S.; Roberts, K. A.; Brinkmeyer, R.; Yeager, C. M.; Santschi, P. H. *Environ. Sci. Technol.* **2011**, *45*, 9975−9983.
(65) Sava, D. F.; Rodriguez, M. A.; Chapman, K. W.; Chupas, P. J.; Greathouse, J. A.; Crozier, P. S.; Nenoff, T. M. *J. Am. Chem. Soc.* **2011**, *133*, 12398−12401.
(66) Chapman, K. W.; Chupas, P. J.; Nenoff, T. M. *J. Am. Chem. Soc.* **2010**, *132*, 8897−8899.
(67) (a) Fox, P. M.; Davis, J. A.; Luther, G. W., III *Geochim. Cosmochim. Acta* **2009**, *73*, 2850−2861. (b) Gallard, H.; Allard, S.; Nicolau, R.; Gunten, U. V.; Croué, J. P. *Environ. Sci. Technol.* **2009**, *43*, 7003−7009.
(68) (a) Boschloo, G.; Gibson, E. A.; Hagfeldt, A. *J. Phys. Chem. Lett.* **2011**, *2*, 3016−3020. (b) Popov, A. I.; Geske, D. H. *J. Am. Chem. Soc.* **1958**, *80*, 1340−1352.
(69) Runde, W. H.; Mincher, B. J. *Chem. Rev.* **2011**, *111*, 5723−5741.